Journal Name

ARTICLE

Efficient one-pot production of γ-valerolactone from xylose over Zr-Al-Beta zeolite: rational optimization of catalyst synthesis and reaction conditions

Received 00th January 20xx,
Accepted 00th January 20xx

DOI: 10.1039/x0xx00000x

www.rsc.org/

Juan A. Melero[a,*], Gabriel Morales[a], Jose Iglesias[a], Marta Paniagua[a], Clara López-Aguado[a], Karen Wilson[b], Amin Osatiashtiani[b]

The one-pot conversion of xylose into γ-gammavalerolactone in 2-propanol over bifunctional Zr-Al-Beta zeolites, prepared via a post-synthetic route, was optimized in terms of both catalyst synthesis and reaction conditions. In the catalyst preparation, the use of $Zr(NO_3)_4$ as zirconium source as well as the tuning of the amount of water used during the impregnation had a strong impact on the activity of the Zr species due to an improved dispersion of Zr species. As for the aluminium to zirconium exchange, an optimal Al/Zr ratio of 0.20 was identified to provide a catalyst with better activity. The modelization of the catalytic system through experimental design methodology allowed to identify the optimal values of the most influential reaction conditions: temperature 190 ºC, catalyst loading 15 $g{\cdot}L^{-1}$, and starting xylose concentration 30.5 $g{\cdot}L^{-1}$. Under these optimized reaction conditions, Zr-Al-Beta catalyst provides a GVL yield from xylose (ca. 34%) after only 10 h. The catalysts are stable and reusable after thermal regeneration at 550ºC.

Introduction

The interest of ɣ-valerolactone (GVL) as a versatile biomass-derived platform chemical has grown fast in the last decade due to its good properties as green solvent and fuel additive, as well as precursor for the production of liquid alkanes and high-value biopolymers [1-10]. The currently proposed strategy for GVL production is a multi-step process starting by the selective fractionation and depolymerization of the lignocellulosic biomass. This is followed by the acid catalyzed transformation of the released monosaccharides into levulinic acid (LA), which is then hydrogenated to the desired GVL, using hydrogen gas, and catalytic bed reactors bearing supported noble-metals (Ru, Pt and Ir). Although this approach has been reported to provide high yields towards GVL, it also has important drawbacks: the use of mineral acids for the acid-catalyzed steps; only hexoses are transformed into GVL; the use of expensive catalysts in the hydrogenation step; and the requirement of high hydrogen pressure (> 30 bar).

As an alternative to the conversion of LA to GVL using H_2 over noble-metals, the reduction of LA and its esters by catalytic transfer hydrogenation (CTH) *via* Meerwein-Ponndorf-Verley (MPV) reaction in the presence of an H-donor alcohol has been widely described in literature [11-12]. This approach offers a high chemo-selectivity for the reduction of carbonyl groups under mild conditions and without the requirement of expensive metals as active phase or high hydrogen pressures (Fig. ESI-1). Zirconium-based catalysts of different nature (ZrO_2, Al_2O_3-ZrO_2, Zr-SBA-15, ZrO_2/SBA-15, $Zr(OH)_4$, ZrFeO, etc.) have been tested for the production of GVL from LA and its esters in the presence of different alcohols (mainly 2-propanol because of its high reactivity in MPV reduction) yielding in most of the catalytic assays GVL yields over 80 % [13-19]. On the other hand, pure-silica zeolites doped with Zr and Sn provide the presence of acid Lewis sites, which efficiently promote the CTH reactions. In this way, Roman-Leshkov *et al* have recently studied the catalytic performance of different Lewis metal-modified zeolites (Zr-Beta, Al-Beta, Sn-Beta and Ti-Beta) in the production of GVL from methyl-levulinate in 2-butanol [20]. Among these zeolites, Zr-beta showed the best catalytic results with a GVL selectivity close to 100 % after 5 hours of reaction and complete levulinate conversion. Later, Wang et al. demonstrated that Zr-Beta zeolite is also a robust and active catalyst for the MPV reduction of levulinic acid to GVL [21]. The high activity of this catalyst was attributed to the presence of Lewis acidic sites with moderate strength coming from the incorporation of zirconium atoms within lattice positions of the zeolite framework.

These studies are focused on the use of LA and/or its esters, but this approach needs a source of high-purity LA. Hence, a great interest has arisen to obtain GVL not from levulinic acid but directly from other available biomass-derived molecules in a one-pot approach through the combined action of acid (Brønsted) and reduction

[a] *Chemical and Environmental Engineering Group, Universidad Rey Juan Carlos. C/ Tulipan s/n, 28933 Móstoles, Madrid (Spain). E-mail: juan.melero@urjc.es.*
[b] *European Bioenergy Research Institute (EBRI), Aston University, Aston Triangle, Birmingham B4 7ET (United Kingdom)*

Electronic Supplementary Information (ESI) available: [details of any supplementary information available should be included here]. See DOI: 10.1039/x0xx00000x

(Lewis) sites, thus avoiding the need of isolating LA. In this way, the group of Roman-Leshkov firstly reported an integrated catalytic process for the efficient production of GVL from furfural in a one-pot process using a physical mixture of Lewis and Brønsted catalysts[20]. In the cascade of reactions, furfural is firstly converted into furfuryl alcohol through a transfer hydrogenation reaction promoted by a Lewis acid catalyst (Zr-Beta zeolite) using 2-butanol as the hydrogen donor. Next, a Brønsted acid catalyst (Al-ZSM-5 zeolite) converts furfuryl alcohol into a mixture of levulinic acid and butyl levulinate through hydrolytic ring-opening reactions. Finally, both levulinic acid and butyl levulinate undergo a second transfer-hydrogenation step, catalyzed again by Zr-Beta, to produce GVL with a yield over 70%.

A step forward has been recently described in several works, aiming to combine Lewis and Brønsted acid sites within the same zeolite framework (bifunctional catalysts). Thus, Winoto *et al* [22] have reported a bifunctional Sn-Al-Beta zeolite for the production of GVL from furfural. Thereby, Lewis acid Sn-Beta zeolites with Brønsted acid Al sites in the framework were synthesized via a post-synthesis procedure based on the partial dealumination of the parent Al-Beta followed by the incorporation of tin species. An optimized Sn-Al-Beta zeolite with a Si/Sn ratio of 63 and a Si/Al ratio of 473 exhibited the highest GVL yield (60%) at 180 ºC in 2-butanol. More recently, Li *et al*[23] have successfully prepared meso-Zr-Al-beta zeolites via a multiple-step post-synthesis strategy with the combination of controlled dealumination, desilication and metal ions incorporation. Under optimized conditions (catalysts and reaction parameters), these materials achieved an outstanding GVL yield of 95% after 24 h of reaction at 120 ºC in the presence of 2-propanol.

Our research group, going a step further, has firstly reported the direct transformation of the parent monosaccharide, i.e. xylose, into GVL through a single reaction step over Zr-Al-beta zeolites [24]. We demonstrated that a proper tuning of the Brønsted/Lewis acid sites ratio is essential to efficiently promote the alternant MPV and acid-driven reaction steps. In this way, a zirconium-modified Beta zeolite with an Al/Zr molar ratio of 0.22 attained a 35 % GVL yield starting from xylose after 48 h at 190 ºC using 2-propanol as H-donor. In this contribution, we have optimized the synthesis conditions of Zr-Al-Beta in order to increase the Zr species dispersion with the purpose of improving the production of GVL from xylose. Likewise, the influence of reaction conditions, including temperature, and catalyst and xylose concentration, has been investigated through an experimental design methodology.

Experimental

Catalysts preparation

The procedure for the synthesis of zirconium-modified Beta zeolites (Zr-Al-Beta) was slightly modified from that reported in literature[21,24]. A commercially available H-Beta zeolite (Si/Al=22) was purchased from Zeolyst International and used as parent support. Partial dealumination was carried out by treatment in nitric acid solution (60% aq. HNO_3, Scharlau), using varying acid concentrations at room temperature (1h, 20 $mL \cdot g^{-1}$). Higher dealumination degrees were achieved using harsher conditions (10M HNO_3, 100 ºC, 20 $mL \cdot g^{-1}$) and increasing times. After washing with deionized water and centrifugation to recover the solid products, the resulting materials were dried overnight (110 ºC). Thereafter, zirconium incorporation was accomplished by incipient wetness impregnation of the dealuminated zeolites with an aqueous solution of the Zr precursor (zirconium oxychloride, Aldrich, or zirconium (IV) nitrate, Chemical Point). The amount of zirconium precursor was adjusted to match that of extracted aluminium. Solvent was removed under vacuum from the resultant slurries, and the solids were dried overnight and then calcined in air at 200 ºC for 6h (3 $ºC \cdot min^{-1}$ heating ramp) and thereafter at 550 ºC for another 6h (same heating rate). The different so-synthesised Zr-modified Beta zeolites were consecutively named as Zr-Al-Beta-*n* (Table 1).

Catalysts characterization

Zirconium and aluminium contents were determined by Inductively Coupled Plasma-Optical Emission Spectroscopy (ICP-OES) with a Varian Vista AX apparatus. Textural properties of the tested catalysts were calculated from argon adsorption-desorption isotherms, which were recorded at 87K using an AutoSorb equipment (Quantachrome Instruments). Average pore size was estimated using the NLDFT method, and total pore volume was taken at P/Po = 0.98. X-ray powder diffraction (XRD) patterns were collected in a Philips X-pert diffractometer using the Cu Kα line in the 2θ angle range from 5º to 65º (step size 0.04º). Transmission electron microscopy (TEM) images were obtained on a PHILIPS TECNAI-20 electronic microscope operating at 200kV. Acid properties of the materials were determined by means of temperature-programmed desorption of NH_3 in a Micromeritics 2910 (TPD/TPR) equipment fitted with a TCD detector. Diffuse reflectance infra-red Fourier transform (DRIFT) spectra were obtained using a Thermo Scientific Nicolet iS50 FT-IR spectrometer with Smart Collector accessory, mid/near infrared source and mercury cadmium telluride (MCT-A) photon detector at -196 °C (liquid N2). All the spectra are average of 64 scans measured at a resolution of 4 cm^{-1}. Samples were diluted homogeneously to 10 wt. % with KBr. For *ex situ* pyridine adsorption, diluted samples were impregnated with neat pyridine, and excess physisorbed pyridine was removed *in vacuo* at 40 °C for 18 h prior to room temperature measurement *in vacuo*. X-ray Photoelectron Spectroscopy (XPS) measurements were obtained using a Specs Phoibos 150 9MCD photoelectron spectrometer.

Catalytic tests

Catalytic tests were typically performed with the reaction composition: catalyst loading 0.01 $g \cdot mL^{-1}$, xylose:2-propanol (Scharlau, 98%) molar ratio 1:50, xylose (XYL) (Sigma Aldrich, 99%) loading 0.026 $mol \cdot g_{CAT}^{-1}$. Catalytic runs were carried out in a stainless steel stirred autoclave (200 mL) with temperature control and pressure gauge. After sealing the reactor, stirring was fixed at 1000 rpm in order to avoid mass transfer hindrances, and a heating rate of 6 $ºC \cdot min^{-1}$ was established to reach the desired temperature within

1 h. This point is taken as the beginning of the reaction, ignoring the time needed for heating up. Decane (Acros Organics >99%) was used as internal standard (0.01 g·mL^{-1}). Samples were withdrawn periodically and filtered into a vial before analysis.

Products analysis

Conversion of xylose was evaluated by HPLC with an Evaporative Light Scattering Detector (ELSD) (Agilent Technologies 1260 Infinity), using a Hi-PLEX H$^+$ column (300 mm-long, 7.7 mm-i.d., 8 µm particle size). Reaction samples were also analysed by gas chromatography (GC), using a Varian 3900 gas chromatograph fitted with a ZB-WAX Plus column (30 m x 0.25 mm, DF=0.25 µm) and a FID detector. Compounds detected by GC were furfural (Sigma Aldrich, 99%), furfuryl alcohol (Sigma Aldrich, 98%), isopropyl furfuryl ether (Manchester Organics, 97%), isopropyl levulinate (iL) (98%, non-commercial, see below for its preparation), levulinic acid (LA) (Sigma Aldrich 98%), α/β-angelica lactones (LACT) (Sigma Aldrich, 98%), γ-valerolactone (GVL) (Sigma Aldrich, 99%) and methyl-β-D-xylopyranoside (Sigma Aldrich, 99%) as a representative of the family of isopropyl xylosides formed by etherification of xylose with 2-propanol. Isopropyl levulinate was synthetized by esterification of levulinic acid in 2-propanol with sulfuric acid as catalyst. Purification of the resultant levulinate was accomplished following a previously described procedure[20]. After removal of 2-propanol by distillation under reduced pressure, the product mixture was dissolved in MTBE and extracted 3 times with saturated aq. $KHCO_3$ solution and 3 times with distilled water. The solution was dried with anhydrous Na_2SO_4 and then filtered. Finally, the solvent was removed by distillation under reduced pressure. Purification grade was assessed by ^{1}H NMR and ^{13}C NMR spectroscopy. ^{1}H NMR (400 MHz, $CDCl_3$): δ 4.97 (sep, J = 6.3 Hz, 1H), 2.72 (t, J = 6.7 Hz, 2H), 2.52 (dt, J = 0.4, 6.7 Hz, 2H), 2.17 (s, 3H), 1.2 (d, J = 6.3 Hz, 6H) ppm; ^{13}C NMR (100 MHz, $CDCl_3$): δ 206.98 ($CH_3C(O)$-); 172.45 (-C(O)OiPr), 68.18 (-$C(CH_2)CH_2$), 38.19 ($CH_3C(O)C$-), 30.07 ($CH_3C(O)CH_2C$-), 28.58 ($CH_3C(O)$-), 21.96 (-$C(CH_2)CH_2$) ppm. The identification of others bio-products, such as 2-propoxy glycol and isopropyl lactate coming from the retro-aldol condensation of xylose (Fig. ESI-2) was checked by GC-MS using a Bruker 320-MS GC Quadrupole Mass Spectrometer equipped with a capillary column (BR-SWax, 30 m x 0.25 mm, DF=0.25 µm), using He as carrier gas. Product quantification was based on a previous calibration of the analysis unit with standard stock solutions of pure commercially-available chemicals using decane as internal standard. Catalytic results are shown either in terms of absolute conversion of xylose (X_{XYL}) or in terms of yields towards the different products (Y_i). The definitions of these parameters are as follows:

$$X_{XYL} = \frac{Reacted\ mol\ of\ xylose}{Initial\ mol\ of\ xylose} \times 100 \quad (1)$$

$$Y_i = \frac{Formed\ mol\ of\ i}{Initial\ mol\ of\ xylose} \times 100 \quad (2)$$

Optimization of the reaction conditions

Response surfaces were calculated to optimize the operation conditions using Al-Zr-Beta zeolite to maximize GVL yield. Three independent operation variables (factors) were selected: the reaction temperature (X_1), the catalyst loading (X_2), and the starting xylose concentration (X_3). Table 1 lists the experimental range for the selected operation variables, which are based on preliminary experimental results[24], as well as the corresponding levels of the factors. A face-centered central composite design consisting of 18 experiments was performed, comprising 8 factorials points, 6 star points, and 4 cube center replicas.

Table 1. Full factorial face-centered composite design matrix of three variables and the observed responses in the optimization of GVL production in presence of Al-Zr-Beta.

Factor		Coded levels		
		-1	0	+1
X_1	Temperature (ºC)	150	170	190
X_2	Catalyst loading (g·L^{-1})	5	10	15
X_3	Starting xylose concentration (g·L^{-1})	10	40	70

All experiments were carried out in a randomized order to minimize the effect of unexplained variability in the observed response. Experimental data were analyzed by response surface methodology using a second-order polynomial equation such as the following one:

$$Y = \beta_0 + \sum_{n=1}^{3} \beta_n \cdot X_n + \sum_{n=1}^{3} \beta_{nn} \cdot X_n^2 + \sum\sum_{n<m}^{3} \beta_{nm} \cdot X_n \cdot X_m \quad (3)$$

where Y is the response (GVL yield, mol%) and β_0, β_n, β_{nn} and β_{nm} are the coefficients of the model, representing the intercept, linear, quadratic, and binary interactions, respectively. X_n and X_m are the studied independent factors. An analysis of variance (ANOVA) was performed to calculate the regression coefficients. The analysis of statistical significance was based on the total error criteria with a confidence level of 95.0%.

Results and discussion

Within this work, we have optimized the synthesis of Zr-modified Beta catalysts in order to maximize the production of GVL in the cascade reaction from xylose. The starting point for this optimization was the catalyst that has so far provided the best performance[24], i.e. Zr-Al-Beta prepared via a post-synthetic dealumination procedure, using zirconium oxychloride as zirconium precursor, with 0.22 Al/Zr ratio, and 0.17 Brønsted/Lewis acid sites ratio. This catalyst was able to provide 22.6 % yield of GVL after 48h at 170ºC, reaching 35 % when increasing the temperature up to 190ºC. The proposed strategies for the optimization of the synthesis have followed two different routes: i) increasing the surface dispersion of Zr species in the dealuminated zeolite, and ii) exploring a further reduction of the Al/Zr ratio, by means of reducing the amount of aluminium. For the first effect, a different zirconium precursor, $Zr(NO_3)_4$, has been

tested. This compound displays higher water solubility than the previously used $ZrOCl_2$ and thus a better dispersion of Zr species during the impregnation can be obtained[25]. In the same line, an increase of water amount during the impregnation step, in order to favour Zr^{4+} ions mobility, has also been evaluated. Finally, lower Al/Zr ratios have been obtained by increasing the harshness of the dealumination procedure (longer refluxing times in concentrated nitric acid solution) while keeping constant the Zr loading.

Considering all these factors, a series of modified Zr-Al-Beta zeolites were prepared and Table 2 summarises their physicochemical properties as well as the GVL yield achieved after 48h at 170ºC. The benefits of using $Zr(NO_3)_4$ vs. $ZrOCl_2$ as zirconium precursor are highlighted when comparing samples Zr-Al-Beta-1 and Zr-Al-Beta-2. Both materials come from the same dealuminated Beta zeolite and have very similar composition and structure, except for the NH_3-TPD analysis that shows a slight decrease in acidity from 0.35 to 0.28 mmolH+/g. TEM analysis (Fig. 1) shows high homogeneity of material Zr-Al-Beta-2, without any evidence of ZrO_2 bulk agglomerates, in consonance with a lattice incorporation of the Zr species. On the contrary, the sample prepared from $ZrOCl_2$ displays some minor small dark contrast areas, indicating some degree of inhomogeneity probably coming from the accumulation of poorly dispersed Zr species. The catalytic evaluation of both samples is depicted in Figure 2. The better zirconium dispersion achieved for Zr-Al-Beta-2 results in an enhancement of the cascade reaction rate, as it can be inferred from the higher final GLV yield (30 % vs 24 %, after 48h). Analysing the evolution of the different species with time, some remarkable aspects highlighting the acceleration of the process towards GVL are the lower 2-propyl xylosides concentration, the better catalytic performance in dehydration reactions, as well as lower contents on furfural and iso-propyl levulinate obtained over Zr-Al-Beta-2. This improvement can be ascribed to an enhancement of both carbonyl groups reductions (MPV transformations) because of a higher activity of the better-dispersed zirconium. As a side effect, the enhancement of Zr sites activity also contributes to increase the extent of the retro-aldol condensation of xylose, providing products such as 2-propyl lactate and 2-propoxyethanol (see Fig. ESI-2), which can be ascribed to a higher Lewis acidity in these materials.

Regarding the structural characterization of the materials included in Table 2, as a general trend, all the samples prepared using zirconium nitrate preserved the typical XRD pattern of the parent Beta zeolite (Fig.ESI-3a). Additionally, typical XRD reflections of crystalline ZrO_2 could not be observed in these materials, indicating the absence of large domains of this metal oxide, and a proper incorporation of Zr into lattice positions within the zeolite structure. Likewise, textural properties measured by argon manometric porosimetry (Fig.ESI-3b) confirm the absence of significant structure damage during the synthesis procedure.

Table 2. Physicochemical properties of the Zr-Al-Beta zeolites and catalytic performance in the production of GVL from xylose.

Catalyst	Zirconium precursor	H_2O[a] ($mL \cdot g^{-1}$)	Composition[b]					BET area[c] ($m^2 g^{-1}$)	Total pore volume[d] ($cm^3 g^{-1}$)	Acidity		Yield to GVL[g] (%)
			% Al	% Zr	Si/Al	Si/Zr	Al/Zr			(mmol $H^+ g^{-1}$)[e]	B/L ratio[f]	
Beta (parent)	-	-	2.0	0.0	22	-	-	623	0.36	0.41	0.56	0
Zr-Al-Beta-1	$ZrOCl_2$	5	0.28	5.0	149	28	0.19	582	0.37	0.35	0.17	24
Zr-Al-Beta-2	$Zr(NO_3)_4$	5	0.27	4.5	156	32	0.20	561	0.36	0.28	0.03	30
Zr-Al-Beta-3	$Zr(NO_3)_4$	5	0.12	4.0	354	36	0.10	601	0.39	0.21	0.04	22
Zr-Al-Beta-4	$Zr(NO_3)_4$	5	0.06	4.5	704	32	0.05	567	0.33	0.18	0.05	14
Zr-Al-Beta-5	$Zr(NO_3)_4$	5	0.04	6.4	1027	22	0.02	559	0.36	0.15	0.07	10
Zr-Al-Beta-6	$Zr(NO_3)_4$	10	0.27	4.5	156	32	0.20	685	0.38	0.29	0.05	37
Zr-Al-Beta-7	$Zr(NO_3)_4$	15	0.23	4.6	183	31	0.17	681	0.38	0.27	0.10	32

[a] Amount of water used during the impregnation of Zr precursor. [b] % Al, % Zr (w/w); Si/Al, Si/Zr, Al/Zr (atomic ratios) measured by ICP-OES. [c] Surface area calculated by the B.E.T. method. [d] Total pore volume recorded at $P/P_0 = 0.975$. [e] Acid sites loading analysed by NH_3-TPD. [f] Brønsted/Lewis acid sites ratio determined by FTIR using pyridine as molecular probe. [g] Yield to γ-valerolactone from xylose; reaction conditions: 170°C, reaction time 48h, xylose:2-propanol molar ratio 1:50, catalyst loading 10 $g \cdot L^{-1}$.

Journal Name

ARTICLE

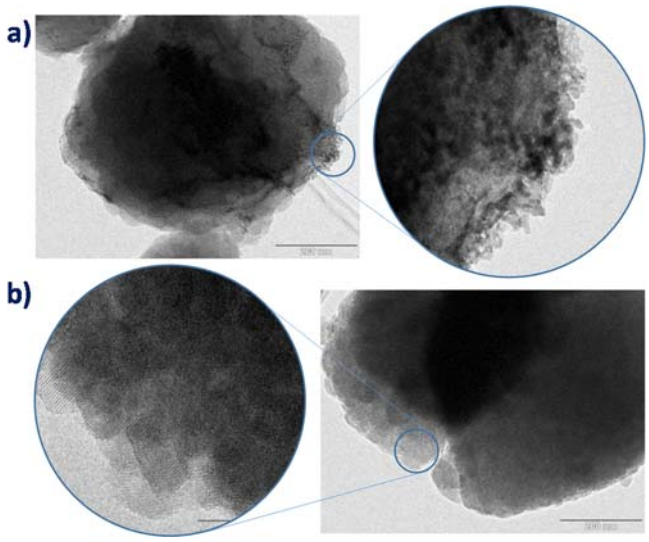

Figure 1. TEM images of (a) Zr-Al-Beta-1 and (b) Zr-Al-Beta-2 zeolites.

Aluminum content was then decreased in order to check the effect of using lower Al/Zr ratios. In this way, materials Zr-Al-Beta-3 to 5 were prepared in the same way than Zr-Al-Beta-2, except for using increasingly harsher dealumination processes. As a result, Al/Zr could be tuned from 0.20 to as low as 0.02 (Table 2). As expected, the higher extent of Al removal from the network, together with an approximately constant Zr loading, resulted in a progressive decrease of the NH_3-TPD acidity of the materials. The assessment of the catalytic activity of these materials resulted in lower final GVL yields, showing a progressive reduction of the production of GVL insofar as the Al content decreases. This result evidences the necessity of a minimum amount of Al sites to effectively catalyze Brønsted acidity reaction steps in the cascade reaction (sugar dehydration, furfuryl alcohol hydration and isomerisation…). On the other hand, samples Zr-Al-Beta-6 and Zr-Al-Beta-7 were prepared using higher water concentrations during the impregnation with zirconium nitrate, double (10 $mL{\cdot}g^{-1}$) and triple (15 $mL{\cdot}g^{-1}$), respectively, than in Zr-Al-Beta-2. Despite the composition, textural and structural properties do not vary significantly among the three samples (indeed, they keep an almost constant Al/Zr ratio), there is a remarkable effect on the catalytic activity. Thus, doubling the amount of water led to 37 % GVL yield, while tripling it had a lower impact on the catalytic performance, leading to 32 % GVL yield.

The relative presence of Brønsted and Lewis acid sites was assessed by means of DRIFT spectroscopy for adsorbed pyridine on each sample (Fig. ESI-4). Table 2 incorporates the obtained Brønsted/Lewis acid sites ratios. Among the different synthesized materials, the use of $Zr(NO_3)_2$ as zirconium precursor seems to lead to B/L ratios lower than when $ZrOCl_2$ is used, even at similar Al y Zr contents (see, e.g., Zr-Al-Beta-1 vs. Zr-Al-Beta-6). As a hypothesis, this could be explained by the better dispersion of Zr species when using the more soluble zirconium nitrate. Thus, a better dispersion of Zr species would cover larger portion of the zeolite surface, affecting in a larger extent the Al environments and possibly decreasing part of the Brønsted acidity.

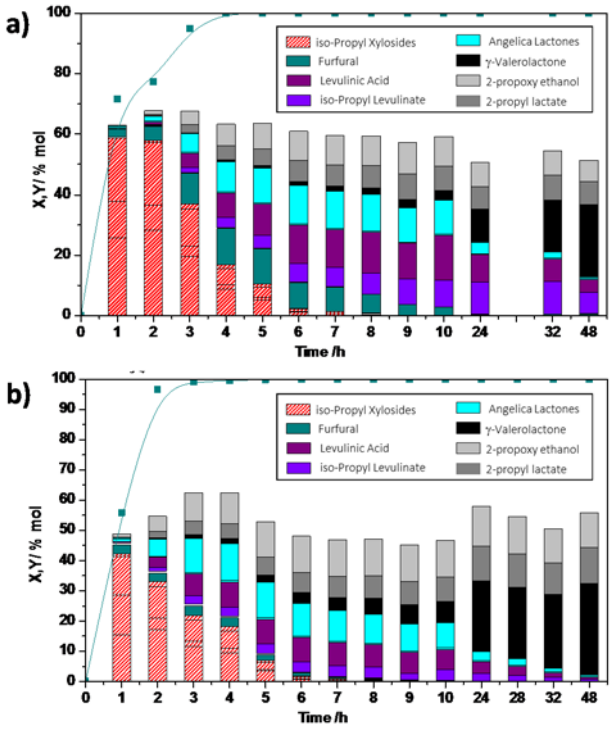

Figure 2. Xylose conversion and yields to products in 2-propanol over a) Zr-Al-Beta-1, b) Zr-Al-Beta-2. Reaction conditions: 170°C, xylose:2-propanol molar ratio 1:50, catalyst loading 10 $g{\cdot}L^{-1}$.

Considering all the above descriptions, it can be concluded that there is an optimal Al/Zr ratio around 0.20 for the production of GVL from xylose over zirconium-modified Beta zeolites. However, this is not the only influential parameter. The zirconium precursor used in the post-synthetic preparation method also results critical, being the zirconium nitrate, a more water-soluble zirconium precursor, more appropriate than the oxychloride counterpart to achieve higher metal dispersions. Furthermore, the amount of water used during the impregnation has an impact on the dispersion of Zr species and,

consequently, on their distributed incorporation within the dealuminated Beta zeolite. Sample Zr-Al-Beta-6 led to the higher yield to γ-valerolactone (Fig. ESI-5) and therefore it was selected to continue with the optimization of the reaction conditions.

Optimization of the reaction conditions

Enhancing the yield towards the desired GVL product requires understanding the influence of the different reaction key factors affecting the progress of the described reaction cascade from xylose to GVL. For this purpose, three operation factors have been varied according to a factorial design of experiments to build a mathematical model that can predict the GVL yield as a function of the reaction conditions. This study not only allows getting a predictive mathematical model to infer the GVL yield, but also studying and get a deep knowledge on the influence of the studied variables on this response factor. Thus, reaction temperature, catalyst loading, and xylose concentration in the reaction medium have been selected as key variables affecting the final GVL yield. For this optimization study, evolution of the reaction media composition was monitored up to 24h. Table 3 lists the experimental face-centered cube design, including the yields to the main products achieved in these catalytic tests.

Table 3. Full factorial face-centered composite design matrix of three variables and the observed responses after 24 h of reaction in the optimization of GVL production over Zr-Al-Beta-6 zeolite.

Run	Experimental factors			Main products yields[d]			
	X_1[a]	X_2[b]	X_3[c]	Y_{iL}	Y_{LA}	Y_{LACT}	Y_{GVL}
1	0	0	0	1.5	1.6	1.3	26.5
2	0	0	0	1.7	1.6	1.6	26.4
3	0	0	0	1.9	1.8	1.8	24.8
4	0	0	0	1.4	1.1	1.2	25.2
5	-1	+1	-1	0.7	0.8	3.4	19.5
6	-1	-1	-1	2.4	5.0	12.5	12.7
7	-1	-1	+1	3.2	6.6	11.3	1.4
8	-1	+1	+1	5.5	9.6	11.1	5.7
9	+1	+1	-1	0.0	0.0	0.0	30.4
10	+1	-1	-1	0.0	0.0	0.0	27.5
11	+1	-1	+1	3.1	3.4	1.8	20.2
12	+1	+1	+1	0.4	0.6	0.3	29.6
13	-1	0	0	5.7	11.0	13.5	10.2
14	+1	0	0	0.2	0.1	0.3	28.8
15	0	-1	0	4.9	6.3	6.0	17.3
16	0	+1	0	0.9	0.6	1.5	30.8
17	0	0	-1	0.2	0.4	0.5	27.3
18	0	0	+1	4.6	6.5	5.6	12.2

[a] Coded temperature; [b] Coded catalyst loading; [c] Coded xylose starting concentration. [d] Yields calculated as (mol produced/mol starting xylose)x100, obtained after 24h of reaction. Products: iL, isopropyl levulinate; LA, levulinic acid; LACT, α/β-angelica lactones; GVL, γ-valerolactone.

The experimental catalytic results were used to test, in a first step, the variability of the analysis procedure by comparing the results obtained in four replicas of the central point (Runs #1-4). Figure 3 depicts the evolution of the products distribution with time, obtained under the reaction conditions corresponding to the center of the experimental field. Repeatability of the catalytic assays is quite high, as it is evident from the comparison of the four different reaction runs depicted in Fig. 3. Actually, reproducibility is better for longer reaction times, as the first stages of the reaction cascade proposed for the transformation of xylose into GVL (etherification, dehydration, H-transfer,…) are quite fast, and slight differences in operational variables like temperature, the catalyst loading or starting xylose concentration, may lead to the larger divergences observed during the early moments of the reaction. Nevertheless, long reaction times, such as 24 h, provide quite similar results in products distribution. In this way, the curvature of the model at 24 h has resulted to be significant for the selected response, the GVL yield.

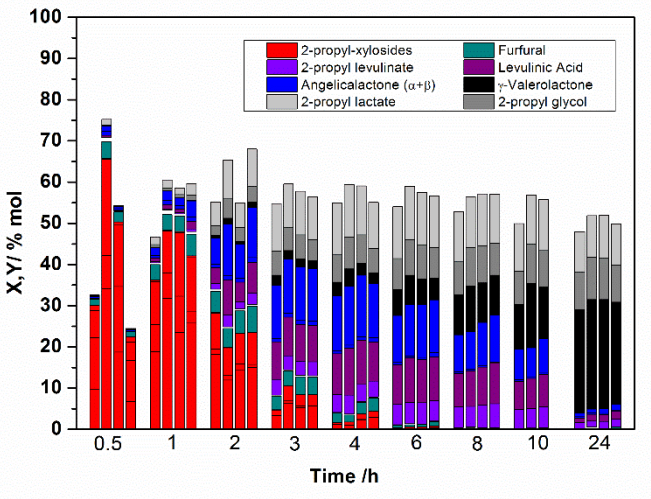

Figure 3. Repeatability of the catalytic test corresponding to the operation conditions at the center of the experimental field: 170ºC, xylose:2-propanol molar ratio 1:50, catalyst loading 0.1 g·mL^{-1}.

A quadratic model was fitted to predict GVL yield as a function of the operation conditions. The mathematical expression, including only the regression coefficients corresponding to significant factors and interactions (at 95% confidence level), is as follows:

$$Y_{GVL}(\%) = 24.5 + 17.4 \cdot X_1 + 7.4 \cdot X_2 - 9.7 \cdot X_3 - 7.5 \cdot X_1^2 - 6.9 \cdot X_3^2 + 4.3 \cdot X_1 \cdot X_3 \quad (4)$$

In this equation, Y_{GVL} represents the GVL yield in mol% units. X_i refers to the independent coded factors, which adopt values between -1 and +1. This mathematical model is valid within the explored experimental region. The value of the regression coefficient, r^2 = 0.9447, indicated a high degree of correlation between the experimentally observed and the predicted values for GVL yield (Fig. ESI-6). Figure 4 depicts the contour plots showing the predicted influence of the operation conditions (temperature, catalyst loading and starting xylose concentration) on the obtained yield towards GVL, based on the generated model. The influence of the distinct operation parameters has been evaluated through the analysis of the

response surfaces depicted in Fig. 4. Thus, the catalyst loading (X_2), though significant, seems to exert a limited influence on the GVL yield. This influence is positive, so that the higher catalyst loading, the higher the GVL yield. However, the influence is linear, which is clearly evident from the equidistant separation of the response surfaces generated at three different catalyst loadings (Fig. 4A). This result is probably a consequence of the studied range of catalyst loadings in quite dilute conditions, thus avoiding the presence of an excessive concentration of solid within the reactor and preventing mass transfer hindrances.

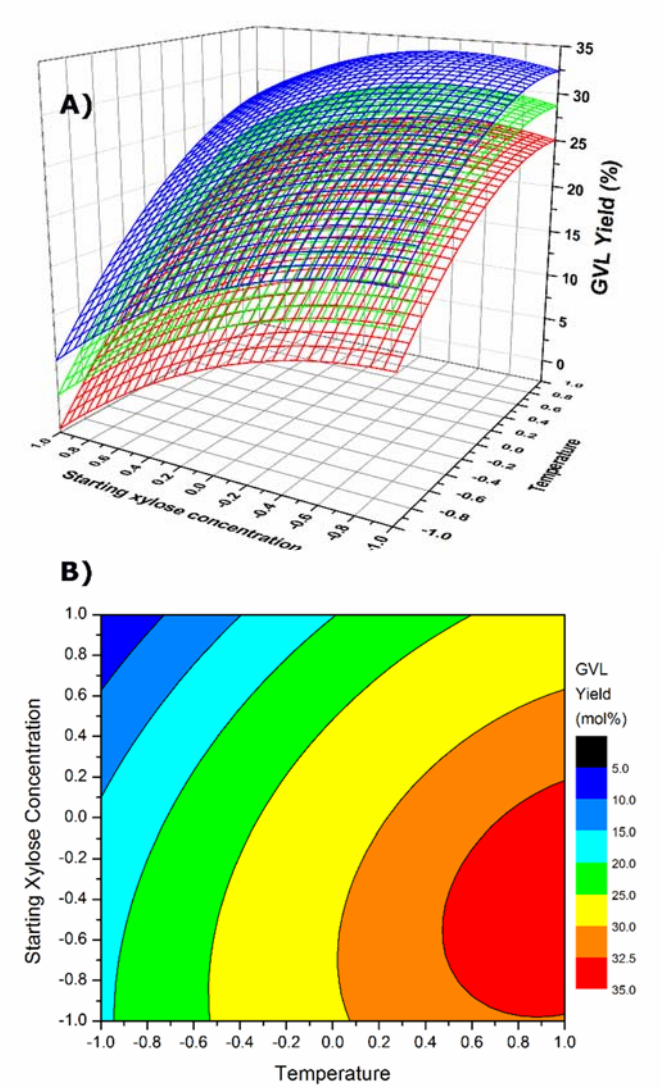

Figure 4. Surface and contour plots obtained for the predicted influence of the operation conditions on the yield to GVL at 24h. A) Surface plots as a function of the catalyst loading (red: 5 g·L^{-1}; green: 10 g·L^{-1}; blue: 15 g·L^{-1}). B) Contour plots representing GVL yield as a function of the starting xylose concentration and the temperature (catalyst loading 15 g·L^{-1}).

As for the influence of the reaction temperature (X_1) and the starting xylose concentration (X_3), both factors play a strong influence, though opposite, on the yield towards GVL. Thus, the reaction temperature exerts a positive influence on the response, because an increase in temperature, accordingly increases the reaction rates of each one of the transformations involved in the proposed reaction cascade (Fig. ESI-7). Thus, elevating the reaction temperature leads to a fast transformation of the starting xylose and its 2-propyl ethers (xylosides), and the rest of the chemical intermediates. However, raising the reaction temperature also leads to an enhanced humins formation, which explains the negative influence of the quadratic term of temperature (Eq. (4)). This is evident from the dark colored solutions obtained when operating at higher temperatures (Fig. ESI-7). Surprisingly, the extension of the retro-aldol condensation reactions seems to be independent on the reaction temperature, as no great differences were observed in the production of 2-propyl lactate and 2-propyl glycol when varying the reaction temperature. Nevertheless, the overall influence of the temperature over the yield towards GVL, under the tested experimental conditions, is positive, as it is clearly visible in Fig.4.

As for the influence of the starting xylose concentration on GVL production, this factor exerts a negative influence on the predicted GVL yield (in both linear and quadratic terms). A detailed analysis of the evolution of the reaction products distribution as a function of the starting xylose concentration (Fig. ESI-8), revealed interesting facts. Thus, lower xylose loadings conducted to higher yields towards the products coming from the retro-aldol condensation of 2-propyl xylosides (2-propyl glycol and 2-propyl levulinate). This suggests that the proposed cascade of reactions from xylose to GVL, through alternate H-transfer reactions and acid driven transformations, is more sensitive to the concentration of the starting sugar than the competing reaction pathway involving the rupture of xylose. On the contrary, the formation of humins seems to be favored when higher concentrations of the starting sugar are used.

Analyzing the complete mathematical model, the maximal predicted value for the yield towards GVL at 24 h within the experimental region is 34.4 mol%. This optimal value corresponds to a reaction temperature of 190ºC, a catalyst loading of 15 g·L^{-1}, and a starting xylose concentration of 30.5 g·L^{-1} (X_1 = +1, X_2 = +1, X_3 = -0.31, in coded values). A catalytic experiment carried out under these reaction conditions over the optimized catalyst (Zr-Al-Beta-6) provided 34.3% Y_{GVL}, in fairly good agreement with the model prediction. Noticeably, under these optimized reaction conditions, the catalyst reaches its maximum value of GVL yield (ca. 34%) already after only 10 h (Fig. ESI-9).

Stability and reusability of the catalyst was evaluated under the optimized reaction conditions. In this way, a hot filtration test discarded the leaching of active metal species to the reaction medium, which could lead to a misleading homogeneous catalysis (Fig. ESI-10). Additionally, for the reutilization experiments, Zr-Al-Beta-6 was recovered by filtration after a first reaction cycle of 24 h. The sample, once dried, presented dark color, which can be attributed to the adsorption of reaction products and non-identified compounds, i.e. humins. In order to remove the organic deposits

from the catalysts surface, a thermal treatment in air (5 h at 550ºC) was applied. Thereafter, the catalyst was used again in a second identical reaction cycle. The procedure was repeated for a third cycle. Figure 5 includes the results in terms of yields to the identified products. As shown, Zr-Al-Beta-6 displayed a very good reusability in the transformation from xylose to GVL, evidencing that the active sites keep their activity essentially intact even after an accumulated reaction time of 72h.

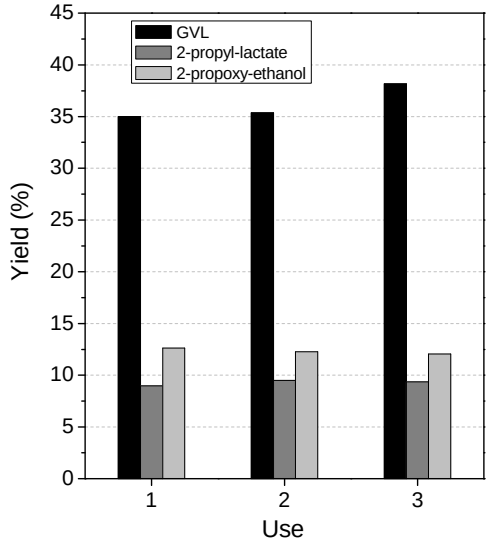

Figure 5. Reutilization of Zr-Al-Beta-6. Yields to products starting from xylose in three consecutive uses with intermediate thermal activation of the catalyst. Reaction conditions: 190ºC, 24h, catalyst loading 15 $g \cdot L^{-1}$, xylose concentration 30.5 $g \cdot L^{-1}$.

Conclusions

Within this work we have shown that for the synthesis of Zr-Al-Beta zeolite, via dealumination and post-synthetic grafting of Zr, there is an optimal Al/Zr ratio around 0.20. Likewise, the use of $Zr(NO_3)_4$ as zirconium source instead of $ZrClO_2$, combined with a proper adjustment of water concentration during the impregnation, allows for an improved catalytic activity in the cascade of reactions from xylose to GVL, which is attributed to a better dispersion of Zr species on the zeolite. Modelling of the catalytic system identified the optimal values of temperature (190 ºC), catalyst loading (15 $g \cdot L^{-1}$), and xylose concentration (30.5 $g \cdot L^{-1}$), in the analyzed experimental range. Under these optimized reaction conditions, the optimized Zr-Al-Beta catalyst reaches its maximum value of GVL yield from xylose (ca. 34%) after only 10 h of reaction. The catalyst showed a good reusability after thermal regeneration in the reaction from xylose, confirming its stability.

Acknowledgements

Financial support from the Spanish Ministry of Economy and Competitiveness through the projects CTQ2014-52907-R and CTQ2015-68844-REDT, as well as from the Regional Government of Madrid through the project S2013-MAE-2882, is gratefully acknowledged. C. López-Aguado thanks the Spanish Ministry of Economy and Competitiveness for a FPI grant (BES-2015-072709).

References

1 J. Q. Bond JQ, D. M. Alonso, D. Wang, R. M. West, J. A. Dumesic, *Science*, 2010, **327**, 1110-1114.
2 J. J. Bozell, *Science*, 2010, **329**, 522-523.
3 J.P. Lange, R. Price, P. M. Ayoub, J. Louis, L. Petrus, L. Clarke, H. Gosselink, *Angewandte Chemie International Edition*, 2010, **49**, 4479-4483.
4 I. T. Horvath, H. Mehdi, V. Fabos, L. Boda, L. T. Mika, *Green Chemistry*, 2008, **10**, 238-242.
5 S. Van de Vyver, Y. Roman-Leshkov, *Catalysis Science & Technology*, 2013, **3**, 1465-1479.
6 K. Yao, C. Tang, *Macromolecules*, 2013, **46**, 1689-1712.
7 D. Fegyverneki, L. Orha, G. Láng, I. T. Horváth, *Tetrahedron*, 2010, **66**, 1078-1081.
8 D. M. Alonso, J. Q. Bond, J. A. Dumesic, *Green Chemistry*, 2010, **12**,1493-1513.
9 R. Palkovits, *Angewandte Chemie International Edition*, 2010, **49**, 4336-4338.
10 K. Yan, Y. Yang, J. Chai, Y. Lu, *Applied Catalysis B: Environmental*, 2015, **179**, 292-304.
11 M. J. Gilkey, B. Xu, *ACS Catalysis*, 2016, **6**, 1420-1436.
12 A. Osatiashtiani, A. F. Lee, K. Wilson, *Journal of Chemical Technology and Biotechnology*, 2017, **92**, 1125-1135.
13 M. Chia, J. A. Dumesic, *Chemical Communications*, 2011, **47**, 12233-12235.
14 X. Tang, H. Chen, L. Hu, W. Hao, Y. Sun, X. Zeng, L. Lin, S. Liu, *Applied Catalysis B: Environmental*, 2014, **147**, 827-834.
15 J. He, H. Li, Y. M. Lu, Y. X. Liu, Z. B. Wu, D. Y. Hu, S. Yang, *Applied Catalysis A: General*, 2016, **510**, 11-19.
16 J. Iglesias, J. A. Melero, G. Morales, J. Moreno, Y. Segura, M. Paniagua, A. Cambra, B. Hernández, *Catalysts*, 2015, **5**, 1911-1927.
17 Y. Kuwahara, W. Kaburagi, Y. Osada, T. Fujitani, H. Yamashita, *Catalysis Today*, 2017, **281**, 418-428.
18 S. S. Enumula, V.R.B. Gurram, M. Kondeboina, D. R. Burri, S.R.R. Kamaraju, *RSC Advances*, 2016, **6**, 20230-20239.
19 H. Li, Z. Fang, S. Yang, *ACS Sustainable Chemistry & Engineering*, 2016, **4**, 236-246.
20 L. Bui, H. Luo, W. R. Gunther, Y. Román-Leshkov, *Angewandte Chemie International Edition*, 2013, **52**, 8022-8025.
21 J. Wang, S. Jaenicke and G. K. Chuah, *RSC Advances*, 2014, **4**, 13481-13489.
22 H. P. Winoto, B. S. Ahn, J. Jae, *Journal of Industrial and Engineering Chemistry*, 2016, **40**, 62-71.
23 G. Wu, W. Dai, N. Guan, L. Li, *Applied Catalysis B: Environmental*, 2017, **205**, 393-403.
24 B. Hernández, J. Iglesias, G. Morales, M. Paniagua, C. López-Aguado, J. L. García-Fierro, P. Wolf, I. Hermans, J. A. Melero, *Green Chemistry*, 2016, **18**, 5777-5781.
25 J. Wang, K. Okumura, S. Jaenicke, G.-K. Chuah, *Applied Catalysis A: General*, 2015, **493**, 112-120.